Realumination of zeolite Y under acidic conditions

Yasunori Oumi[a)], Jou Takahashi[b)], Kazuyoshi Takeshima[b)], Hery Jon[a)], Tsuneji Sano[a),*]

a) Department of Applied Chemistry, Graduate School of Engineering, Hiroshima University, Higashi-Hiroshima 739-8527, Japan ; E-mail: tsano@hiroshima-u.ac.jp

b) School of Materials Science, Japan Advanced Institute of Science and Technology, Tatsunokuchi, Ishikawa 923-1292, Japan

Abstract

Dealuminated zeolites Y were treated with aqueous solutions of various acids and ammonium salts to investigate the realumination behavior under acidic conditions. From the results of ^{27}Al MAS NMR, ^{29}Si MAS NMR and FT-IR measurements, it was found that a part of non-framework aluminum species in the dealuminated zeolite Y is effectively reinserted into the zeolite framework in CH_3COONH_4 and $C_6H_5COONH_4$ aqueous solutions. Pyridine adsorption experiments also revealed that most of incorporated aluminum species generate tetrahedrally coordinated framework aluminum species, namely Brönsted acid sites. Although the realumination also proceeded in H_2SO_4 and CH_3COOH aqueous solutions, large amounts of incorporated aluminum species were not necessarily responsible for generation of Brönsted acid sites. Framework connected aluminum species, presumably as 3-fold-coordinated Lewis acidic framework aluminum species, were mainly generated. In the TEM image of the realuminated zeolite Y, needle-like crystals with ca. 25-80 nm in length were observed, which are probably due to AlOOH generated from non-framework aluminum species.

Keywords Zeolite Y, Dealumination, Realumination, Ammonium salt

1. Introduction

The physicochemical properties of zeolite such as thermal stability and adsorptive, ion-exchange and catalytic abilities are greatly influenced by the content of tetrahedrally coordinated aluminum species in the zeolite framework. Alumination and/or realumination as well as dealumination of zeolite by various treatments have therefore been a matter of considerable interest. The dealumination methods such as thermal, hydrothermal or mineral acid treatments and their mechanisms have been investigated in depth to obtain zeolites with the higher stability and stronger acidity [1-2]. However, the reverse process, alumination and/or realumination, has not been widely studied. Although there are several papers concerning realumination of dealuminated zeolites, the realumination was mainly conducted in the alkaline media [3-11]. Nevertheless, in the alkaline media, dissolution of a part of zeolite framework has been pointed out by several researchers. Therefore, the clarification of dealumination and realumination behaviors of zeolites has been still a matter of scientific and industrial interests.

Recently, we have investigated the reversibility of dealumination-realumination process of several zeolites such as zeolites MOR, MFI, FER and BEA by the pH control method [12-15]. Aluminum species in the solution, which were eliminated from the frameworks of zeolites BEA and MOR by HCl treatment, were easily reinserted into the frameworks under acidic conditions. The amount of incorporated aluminum species increased while the pH value of solutions was 5-6. However, in the case of zeolite MOR, most of incorporated aluminum species were not necessarily responsible for generation of tetrahedrally coordinated framework aluminum sites. Reinsertion of non-framework aluminum species into the dealuminated zeolites MFI and FER hardly occurred.

In order to get further information concerning the realumination process under acidic conditions, thus we investigated the realumination behavior of zeolite Y (FAU), one of industrially important zeolites as solid acid catalyst, in this paper.

2. Experimental section

2. 1. Dealumination and realumination of zeolite Y

Zeolite NH_4Y (SiO_2/Al_2O_3 ratio of 5.5) from Catalysts & Chemicals Ind. Co. (Japan) was used as the parent zeolite. The dealuminated zeolite Y was prepared by steaming the zeolite NH_4Y at 400°C for 20 min. Realumination of the dealuminated zeolite Y was carried out using aqueous solutions of H_2SO_4, CH_3COOH and several ammonium salts. The detailed realumination conditions are listed in Tables 1 and 2. Namely, 5 g of the dealuminated zeolite Y was suspended in water and then a certain amount of 0.025 M H_2SO_4 and CH_3COOH aqueous solutions or 2 M ammonium salt aqueous solution was added to the suspension, whose pH value was controlled in the range from 3 to 6. The suspension was stirred at 75-150°C for 0.5-72 h. The product was filtered off, washed thoroughly with hot deionized water (60°C) and dried at 120°C for 12 h.

2. 2. Characterization

The identification of zeolites obtained was achieved by X-ray diffraction (XRD, Rigaku RINT 2000). The bulk chemical composition was measured by X-ray fluorescence (XRF, Philips PW2400). Textural properties were determined by N_2 adsorption (Bel Japan Belsorp 28SA). Before adsorption measurements at -196°C, the powdered samples (ca. 0.1 g) were evacuated at 400°C for 4 h. ^{27}Al and ^{29}Si MAS NMR spectra were recorded on a Varian VXP-400 spectrometer with 4 kHz spinning speed at 104.3 MHz and 1.73 μs pulses for 4000 scans and at 79.5 MHz and 7.5 μs pulses for 2000 scans, respectively. Aluminum nitrate

nonahydrate and tetramethylsilane were used as chemical references. Prior to the ^{27}Al MAS NMR measurements, the sample was moisture-equilibrated on a saturated solution of NH_4Cl for 24 h. The IR spectra for the framework vibration were recorded on a FT-IR spectrometer (JEOL JIR-7000) with a resolution 4 cm^{-1} at room temperature. The sample was pressed into a self-supporting thin wafer (ca. 6.4 mg cm^{-2}) and was placed in a quartz IR cell with CaF_2 windows. Prior to the measurements, each sample was dehydrated under vacuum at 400°C for 2 h. The IR spectra of chemisorbed pyridine on various zeolites Y were also measured at room temperature. The adsorption of pyridine was carried out at 150°C for 1 h, and then evacuated at 200°C for 30 min to remove the excess and weakly adsorbed pyridine. High-resolution transmission electron microscope (TEM) images were obtained on a Hitachi H-9000 NAR microscope with an accelerating voltage of 300 kV.

3. Results and discussion

3.1. Realumination in H_2SO_4 and CH_3COOH aqueous solutions

At first, the dealuminated zeolite Y prepared by steaming was characterized. The XRD pattern of the dealuminated zeolite showed no peaks other than those corresponding to FAU structure and then the intensities of the peaks observed were almost the same as those of the parent zeolite, indicating no structural degradation. The framework SiO_2/Al_2O_3 ratio calculated from the ^{29}Si MAS NMR spectrum (not shown here) was larger than the bulk SiO_2/Al_2O_3 ratio obtained by XRF analysis. As it is well recognized that the framework SiO_2/Al_2O_3 ratio obtained from the ^{29}Si MAS NMR spectrum cannot be regarded as an accurate value when a lot of silanol groups, i.e. structural defect $SiOH(OSi)_3$, are present in the dealuminated zeolite. The silanol species give a peak at ca. -100 ppm and this peak coincides with that of the $Si(1Al)(OSi)_3$ that is also found at ca. -100 ppm. However, there was no enhancement in the -100 ppm peak in the ^{1}H-^{29}Si cross polarization (CP) MAS NMR

spectrum, indicating smaller amounts of silanol species in the dealuminated zeolite Y. Therefore, the aluminum species removed from the zeolite framework were found to remain in the zeolite as non-framework aluminum species. Presumably, the aluminum species may be connected to the zeolite framework only by one or two remaining chemical bonds [16,17].

Next, the possibility of reinsertion of the non-framework aluminum species into the FAU framework under acidic conditions was investigated. The dealuminated zeolite Y was suspended in water and then the pH value of the suspension was varied from 3 to 6 by adding 0.025 M H_2SO_4 or CH_3COOH aqueous solutions. Table 1 lists the characteristics of zeolites Y obtained with various pH values. Except for the zeolite Y obtained at pH 3.0, the BET surface area and pore volume were similar to those of the parent zeolite, indicating that the zeolite framework structure is maintained even after the acid treatment. In the case of the treatment with H_2SO_4, the framework SiO_2/Al_2O_3 ratio calculated by ^{29}Si MAS NMR spectrum was slightly smaller than that of the dealuminated zeolite and a slight increase in the unit cell parameter was observed. On the other hand, in the case of the treatment with CH_3COOH as weak acid, the framework SiO_2/Al_2O_3 ratio became smaller as compared to the treatment with H_2SO_4 and a further increase in the unit cell parameter was also observed. The unit cell parameter became close to that of the parent zeolite. As an expansion of the unit cell parameters is related to an increase in the framework aluminum concentration, these results strongly suggest the reinsertion of non-framework aluminum species into the zeolite framework during the CH_3COOH treatment. In addition, silicon and aluminum concentrations of solutions after the treatment as determined by ICP were below 0.1 atom%. This means that there is no zeolite framework dissolution during the treatment under acidic conditions.

To clarify the chemical state of incorporated aluminum species, ^{27}Al MAS NMR spectra of the realuminated zeolites were measured. Figure 1 shows the ^{27}Al MAS NMR spectra of various zeolites Y. The peak intensity was normalized based on 1 g of zeolite. The single

sharp peak assigned to the tetrahedrally coordinated aluminum species was observed at ca. 60 ppm for all samples. The considerable increase in the peak intensity at 60 ppm was observed for the zeolite Y obtained by the treatment with CH_3COOH aqueous solution as compared to the dealuminated zeolite. The peak intensity of the zeolite Y after the CH_3COOH treatment was nearly 60% of the parent zeolite. These results also indicate that a part of non-framework aluminum species present in the dealuminated zeolite Y are reinserted into the zeolite framework under acidic conditions.

It is well known that Brönsted acid sites are generated if the incorporated aluminum species are present in the zeolite framework as tetrahedrally coordinated aluminum species. To get further information concerning reinsertion of aluminums, therefore, the IR spectra in the region of 4000-3000 cm^{-1} of the realuminated zeolites Y were measured (Fig. 2). In the FT-IR spectrum of the protonated zeolite Y prepared from the zeolite NH_4Y under vacuum at 400°C (Fig. 2-(c)), the peaks assigned to the acidic bridged OH of Si(OH)Al in α- and β-cages of FAU framework were clearly observed at ca. 3550 and 3630 cm^{-1}, respectively [18]. Moreover, very weak peaks were observed at ca. 3745 and 3697 cm^{-1}, which are assigned to the isolated silanol group and non-framework aluminum species, respectively. On the other hand, in the FT-IR spectrum of the dealuminated zeolite Y (Fig. 2-(a)), the intensities of these peaks at ca. 3550 and 3630 cm^{-1} markedly decreased and then two weak peaks also appeared at ca. 3681 and 3592 cm^{-1}, which may be due to non-framework aluminum species. As can be seen in Fig. 2-(b), an increase in the intensities of the peaks ca. 3550 and 3630 cm^{-1} were hardly observed for the dealuminated zeolites Y treated with CH_3COOH aqueous solution, indicating no significant increase in Brönsted acid sites by the acid treatment. This fact was not parallel to the ^{27}Al MAS NMR result described above, indicating that most of reinserted aluminums are responsible for generation of framework connected aluminum sites. Thus, the increase in the intensity of the 60 ppm peak assigned to tetrahedrally coordinated aluminum

species may be due to the coordination of one water molecule on the framework connected aluminum species in which one Al-O bond is ruptured, being 3-fold-coordinated Lewis acidic aluminum species that can bind water molecule.

3.2. Realumination in aqueous solution of ammonium salt

In general, in the ^{27}Al MAS NMR spectra of activated zeolites, several peaks originated from framework and non-framework aluminum species are observed. It should be pointed out here that non-framework aluminum species can be classified into framework connected aluminum species which can bind water or ammonia molecule and extra-framework aluminum species which are removed completely from the zeolite framework. Several research groups have already reported the interesting results concerning the reversible changes of these aluminum species in zeolite. Ammonia and water adsorption on dehydrated zeolite was found to be able to convert the coordination of non-framework aluminum species back into a tetrahedral coordination [19-23]. Moreover, since the zeolite with lower SiO_2/Al_2O_3 ratio (i.e. higher acid site density) does not possess thermal stability, it is believed that acidic protons in zeolite contribute to the appearance of octahedrally coordinated aluminums species (framework collapse).

To improve the realumination efficiency, therefore, the dealuminated zeolite Y was treated with 2 M aqueous solutions of various ammonium salts instead of CH_3COOH aqueous solution. Characteristics of zeolites Y obtained are listed in Table 2. Figure 3 shows the XRD patterns of zeolites treated with various ammonium salts together with the parent and the dealuminated zeolites. There was no peak other than those corresponding to FAU structure for all samples. As the intensities of the peaks observed were almost the same as those of the parent zeolite, namely no structural degradation was found to undergo. The unit cell parameter of zeolite obtained was strongly dependent upon the ammonium salt used and the

larger values were obtained for the dealuminated zeolites Y treated with CH_3COONH_4 and $C_6H_5COONH_4$. It demonstrated that the realumination of dealuminated zeolite Y takes place effectively in aqueous solutions of CH_3COONH_4 and $C_6H_5COONH_4$. This was also confirmed from a decrease in the framework SiO_2/Al_2O_3 ratios calculated from the ^{29}Si MAS NMR spectra.

To reveal the chemical state of incorporated aluminum species in the realuminated zeolite, ^{27}Al MAS NMR and FT-IR spectra of the realuminated zeolites were also measured. Figure 4 shows the ^{27}Al MAS NMR spectra of various zeolites Y. For zeolites Y treated with CH_3COONH_4 and $C_6H_5COONH_4$, a considerable increase in the intensity of the peak at ca. 60 ppm was observed, which is assigned to the tetrahedrally coordinated framework aluminum species. Figure 5 shows FT-IR spectra of the zeolites Y realuminated with CH_3COONH_4 and $C_6H_5COONH_4$ together with the parent and the dealuminated zeolites. The significant restoration of the intensities of the peaks at ca. 3550 and 3630 cm^{-1} assigned to the acidic bridged OH of Si(OH)Al in α- and β-cages was remarked, indicating the regeneration of Brönsted acid sites. Therefore, it may be concluded that the realumination of the dealuminated zeolite Y proceeds effectively during the treatment with CH_3COONH_4 and $C_6H_5COONH_4$.

To confirm further regeneration of Brönsted acid sites by the treatment, the acidic property of the realuminated zeolite was examined with IR spectra of adsorbed pyridine. Figure 6 shows the FT-IR spectra of pyridine adsorbed on the parent, the dealuminated and the realuminated zeolites Y in the region of 1650-1400 cm^{-1}. For a reference, the FT-IR spectrum of pyridine adsorbed on the zeolite Y realuminated with CH_3COOH was also depicted. The parent zeolite exhibited several peaks due to pyridinium ion on Brönsted acid sites (B : 1546 and 1641 cm^{-1}), pyridine coordinated to Lewis acid sites (L : 1618 and 1456 cm^{-1}) and hydrogen bonded pyridine (H : 1446 and 1596 cm^{-1}). A peak at 1492 cm^{-1} can be assigned to

pyridine associated with both Brönsted and Lewis acid sites [24]. For the dealuminated zeolite Y, the peaks due to adsorbed pyridines were hardly observed. On the other hand, for the zeolite Y realuminated with CH_3COOH, although the peaks due to pyridinium ion on Brönsted acid sites were observed, the stronger peak due to pyridine coordinated to Lewis acid sites was observed at 1454 cm^{-1}. However, the 1454 cm^{-1} peak due to pyridine coordinated to Lewis acid sites was hardly observed for the zeolites Y realuminated with CH_3COONH_4 and $C_6H_5COONH_4$, indicating that most of reinserted aluminum species are responsible for formation of tetrahedrally coordinated framework aluminum species, namely Brönsted acid sites. Therefore, it was found that the treatment with CH_3COONH_4 and $C_6H_5COONH_4$ is very effective for realumination of the dealuminated zeolite Y. As can be seen in Figs. 4 and 5, however, the realumination efficiency only can reach up to 60%, suggesting the formation of extra-framework aluminum species such as AlOOH, $Al(OH)_3$ or Al_2O_3 in the zeolitic pores. Therefore, the TEM images of the dealuminated and the realuminated zeolites Y were measured. As shown in Fig. 7, bright spot-like regions were observed in addition to the lattice structure for the dealuminated zeolite. The bright spot-like regions are assigned to the mesopores formed by dealumination [25]. On the other hand, the needle-like crystals with ca. 25-80 nm in length, pointed out by two circles in Fig. 7-(B), as well as those regions were observed for the realuminated zeolite. Although the diffraction peaks assigned to AlOOH were not detected in the XRD pattern, the needle-like crystals were presumably AlOOH as judged by the morphology of crystals, which were not reinserted back into the zeolite framework during the realumination treatment.

Furthermore, in order to get better understanding of the realumination with ammonium salt, the dealuminated zeolite Y was treated using CH_3COOH/NH_4OH and CH_3COOH/tetramethylammonium hydroxide (TMAOH) aqueous solutions instead of CH_3COONH_4 aqueous solution. The pH value of the suspension was fixed at 6. As shown in

Fig. 8, the peaks due to the acidic bridged OH of Si(OH)Al in α- and β-cages of zeolite Y recovered considerably when the dealuminated zeolite was treated with CH_3COOH/NH_4OH aqueous solution. However, the realumination hardly occurred in the CH_3COOH/TMAOH system. Although the exact reason why NH_4^+ cation is more effective than TMA^+ cation is not clarified at the present time, it might be due to a difference in the cation size. However, it was clearly indicated that the realumination of the dealuminated zeolite Y is strongly enhanced by addition of base molecules. This was consistent with the results reported in literature [19-23]. The existence of protons in the lattice of zeolite Y severely seems to disturb the changes of framework connected aluminum species into the tetrahedrally coordinated framework aluminum species.

4. Conclusions

From all results described above, it was found that a part of non-framework aluminum species in the dealuminated zeolite Y is effectively reinserted into the zeolite framework in CH_3COONH_4 and $C_6H_5COONH_4$ aqueous solutions. Most of incorporated aluminum species generated tetrahedrally coordinated framework aluminum species, namely Brönsted acid sites. Although the realumination also proceeded in CH_3COOH aqueous solution, large amounts of incorporated aluminum species were not necessarily responsible for generation of Brönsted acid sites. Framework connected aluminum species, probably as 3-fold-coordinated Lewis acidic sites, were mainly generated.

Acknowledgment

The authors gratefully acknowledge Mr. M. Ushio and Mr. R. Kuroda (Catalysts & Chemicals Ind. Co. Ltd. Japan) for providing zeolite NH_4Y and helpful discussion.

References

1. J. Datka, S. Marschmeyer, T. Neubauer, J. Meusinger, H. Papp, F.–W. Schüyze, and I. Szpyt, J. Phys. Chem. **100**, 14451 (1996).
2. M.R. Apelian, A.S. Fung, G.J. Kennedy, and T.F. Degnan, J. Phys. Chem. **100**, 16577 (1996).
3. D.W. Breck and G.W. Skeels, in: L.V.C. Rees (Ed.), Proc. 5th Int. Zeolite Conf., Heyden, London, (1980) p.335.
4. X. Lin, J. Klinowski, and J.M. Thomas, J. Chem. Soc., Chem. Commun. 582 (1986).
5. L. Aouali, J. Jeanjean, A. Dereifn, P. Tougne, and D. Delafosse, Zeolite **8**, 517 (1988).
6. H. Hamdan, B. Sulikowski, and J.M. Thomas, J. Phys. Chem. **93**, 517 (1989).
7. Z. Zhang, X. Liu, Y. Xu, and R. Xu, Zeolites **11**, 232 (1991).
8. H. Ishida and Y. Fukuoka, Nippon Kagaku Kaishi 690 (1994).
9. J. Datka, B. Sulikowsk, and B. Gil, J. Phys. Chem. **100**, 11242 (1996).
10. C. Yang and Q. Xu, Zeolites **18**, 162 (1997)
11. X. Zaiku, C. Qingling, Z. Chengfang, B. Jiaqing, and C. Yuhua, J. Phys. Chem. B **104**, 2853 (2000).
12. T. Sano, R. Tadenuma, Z.B. Wang, and K. Soga, J. Chem. Soc., Chem. Commun. 1945 (1997).
13. T. Sano, Y. Uno, Z.B. Wang, C.–H. Ahn, and K. Soga, Microporous Mesoporous Mater. **31**, 89 (1999).
14. Y. Oumi, R. Mizuno, K. Azuma, S. Nawata, T. Fukushima, T. Uozumi, and T. Sano, Microporous Mesoporous Mater. **49**, 103 (2001).
15. Y. Oumi, S. Nemoto, S. Nawata, T. Fukushima, T.Teranishi, and T. Sano, Mater. Chem. Phys. **78**, 551 (2002).
16. E. Loeffiner, U. Lohse, C. Peuker, G. Oehlmann, L.M. Kustov, V.L. Zholobenko, and V.B.

Kazansky, Zeolites **10**, 266 (1990).

17. I. Kiricsi, C. Flego, G. Pazzuconi, W.O. Parker, R. Millini Jr., C. Perego, and G. Bellussi, J. Phys. Chem. **98**, 4627 (1994).
18. J. Datka, B. Sulikowski, and B. Gil, J. Phys. Chem. **100**, 11242 (1996).
19. E. Bourgeat-Lami, P. Massiani, F.D. Renzo, P. Espiau, and F. Fajula, Appl. Catal. **72**, 139 (1991).
20. B.H. Wouters, T.-H. Chen, and P.J. Grobet, J. Am. Chem. Soc. **120**, 11419 (1998).
21. A. Omegna, J.A. van Bokhoven, and R. Prins, J. Phys. Chem. B **107**, 8854 (2003).
22. J. Jiao, S. Altwasser, W. Wang, J. Weitkamp, and M. Hunger, J. Phys. Chem. B **108**, 14305 (2004).
23. B. Xu, F. Rotunno, S. Bordiga, R. Prins, and J. A. van Bokhoven, J. Catal. **241**, 66 (2006).
24. T. Barzetti, E. Selli, D. Moscotti, and L. Forni, J. Chem. Soc., Faraday Trans. **92**, 1401 (1996).
25. K. Sato, Y. Nishimura, N. Matsubayashi, M. Imamura, and H. Shimada, Microporous Mesoporous Mater. **59**, 133 (2003).

Table 1

Characteristics of zeolites Y realuminated using H_2SO_4 and CH_3COOH.

Sample no.	Realumination conditions				SiO_2/Al_2O_3 ratio		Unit cell parameter /Å	BET surface area /m^2g^{-1}	Pore volume /cm^3g^{-1}
	Acid	pH	Temp. /°C	Time /h	XRF	^{29}Si MAS NMR			
1	H_2SO_4	3.0	75	0.5	Amorphous				
2	H_2SO_4	4.0	75	0.5	5.5				
3	H_2SO_4	5.0	75	0.5	5.4	8.3	24.64±0.004	775	0.29
4	H_2SO_4	5.0	150	48	5.5	8.2	24.64±0.004	775	0.27
5	CH_3COOH	5.1	150	48	5.5	6.8	24.64±0.003		
6	CH_3COOH	6.1	150	48	5.5	6.4	24.65±0.002	778	0.28
7	Parent NH_4Y				5.5	5.0	24.66±0.002	866	0.34
8	Dealuminated Y				5.4	8.8	24.62±0.002	799	0.29

Table 2

Characteristics of zeolites Y realuminated using various ammonium salts.

Sample no.	Realumination conditions				SiO_2/Al_2O_3 ratio		Unit cell parameter /Å	BET surface area /m^2g^{-1}	Pore volume /cm^3g^{-1}
	Acid	pH	Temp. /°C	Time /h	XRF	^{29}Si MAS NMR			
9	NH_4F	8.8	150	48	Amorphous				
10	NH_4Cl	4.3	150	48	5.4	7.9	24.61±0.002	776	0.25
11	NH_4Br	4.2	150	48	5.6	6.7	24.63±0.002	805	0.29
12	NH_4NO_3	4.3	150	48	5.6	7.9	24.62±0.002	764	0.25
13	$(NH_4)_2SO_4$	4.7	150	48	5.5	8.0	24.63±0.004	789	0.30
14	$HCOONH_4$	6.0	150	48	5.6	6.1	24.64±0.002	792	0.29
15	CH_3COONH_4	6.6	150	48	5.6	6.4	24.65±0.001	857	0.31
16	$C_6H_5COONH_4$	6.8	150	48	6.0	6.5	24.65±0.002	881	0.32

Figure captions

Fig. 1 ^{27}Al MAS NMR spectra of various zeolites Y. (a) dealuminated Y (No. 8), (b) Y realuminated with CH_3COOH (No. 6) and (c) the parent zeolite (No. 7).

Fig. 2 FT-IR spectra of various protonated zeolites Y. (a) dealuminated Y (No. 8), (b) Y realuminated with CH_3COOH (No. 6) and (c) the parent zeolite (No. 7).

Fig. 3 XRD patterns of various zeolites Y. (a) dealuminated Y (No. 8), (b) Y realuminated with NH_4NO_3 (No. 12), (c) Y realuminated with CH_3COONH_4 (No. 15), (d) Y realuminated with $C_6H_5COONH_4$ (No. 16) and (e) the parent zeolite (No. 7).

Fig. 4 ^{27}Al MAS NMR spectra of zeolites Y realuminated with various ammonium salts. (a) dealuminated Y (No. 8), (b) NH_4Cl (No. 10), (c) NH_4Br (No. 11), (d) NH_4NO_3 (No. 12), (e) $(NH_4)_2SO_4$ (No. 13), (f) $HCOONH_4$ (No. 14), (g) CH_3COONH_4 (No. 15), (h) $C_6H_5COONH_4$ (No. 16) and (i) the parent zeolite (No. 7).

Fig. 5 FT-IR spectra of various protonated zeolites Y. (a) dealuminated Y (No. 8), (b) Y realuminated with CH_3COONH_4 (No. 15), (c) Y realuminated with $C_6H_5COONH_4$ (No. 16) and (d) the parent zeolite (No. 7).

Fig. 6 FT-IR spectra of pyridine adsorbed on various zeolites Y. (a) dealuminated Y (No.8), (b) Y realuminated with CH_3COOH (No. 6), (c) Y realuminated with CH_3COONH_4 (No. 15), (d) Y realuminated with $C_6H_5COONH_4$ (No. 16) and (e) the parent zeolite (No. 7). B and L

denote Brönsted and Lewis bound pyridines, respectively. H denotes hydrogen bonded pyridine.

Fig. 7 TEM images of (A) dealuminated Y (No. 8) and (B) Y realuminated with CH_3COONH_4 (No. 15).

Fig. 8 FT-IR spectra of protonated zeolites Y realuminated with (a) CH_3COOH (No. 6), (b) CH_3COOH/TMAOH and (c) CH_3COOH/NH_4OH.

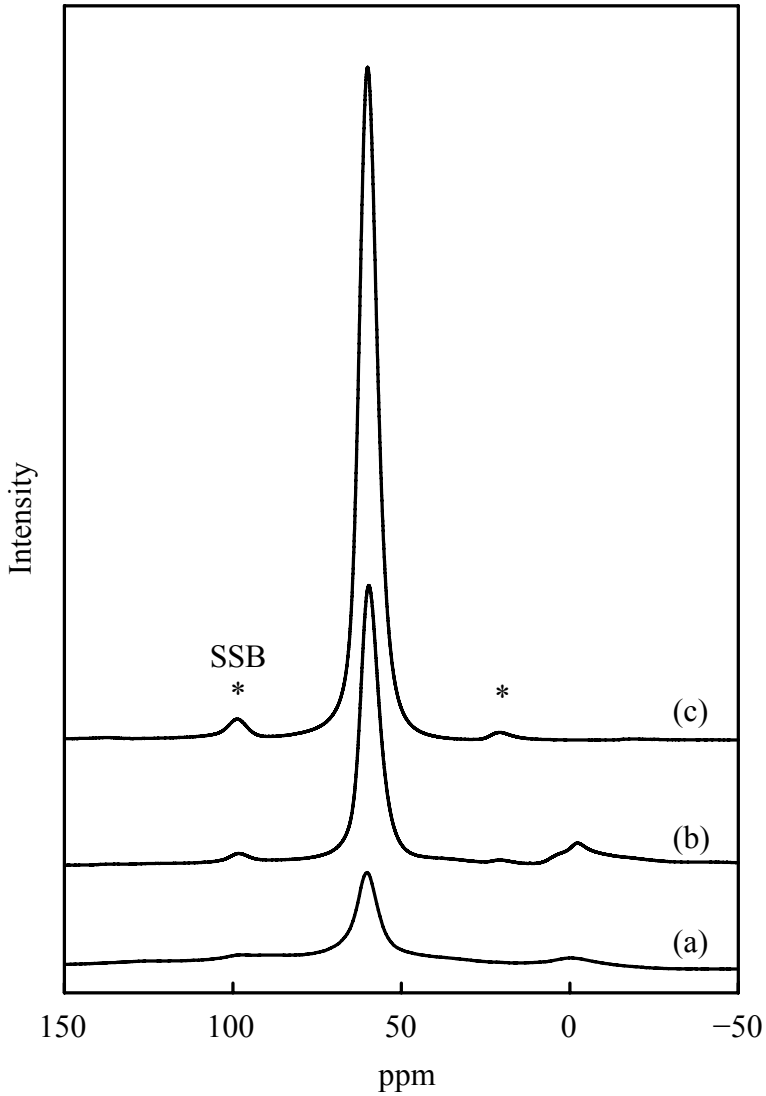

Fig. 1

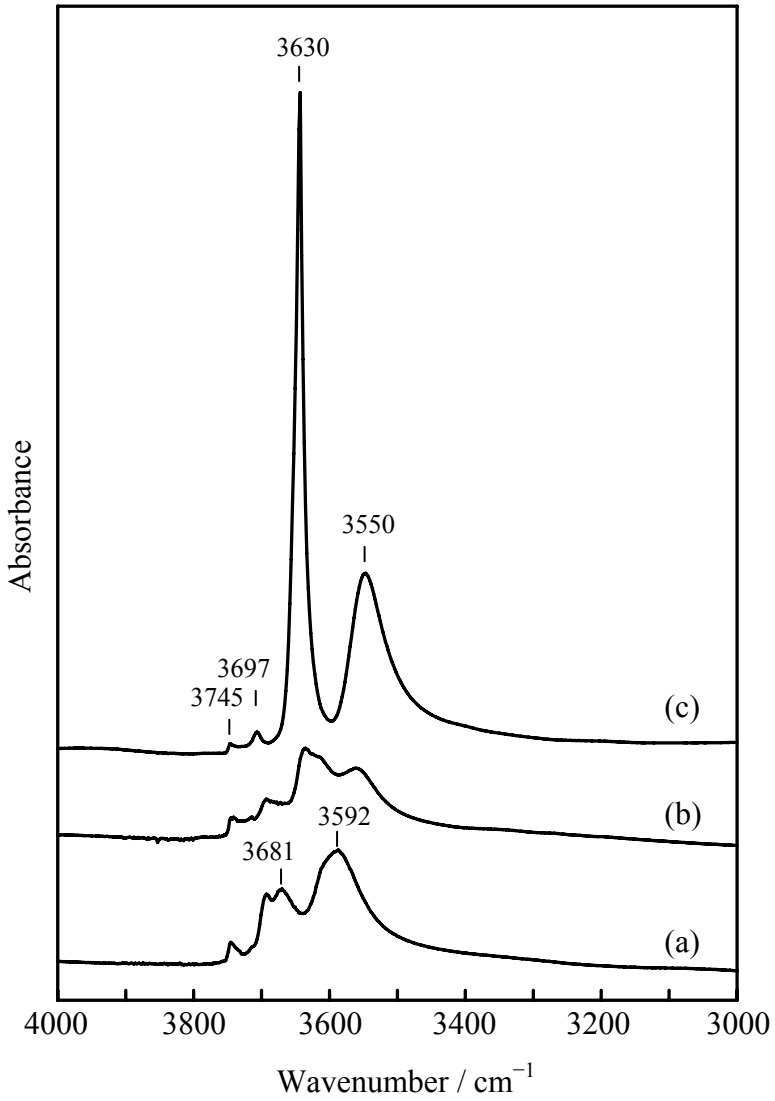
3630
3550
3697
3745
(c)
(b)
3592
3681
(a)
Absorbance
4000
3800
3600
3400
3200
3000
Wavenumber / cm^{-1}

Fig. 2

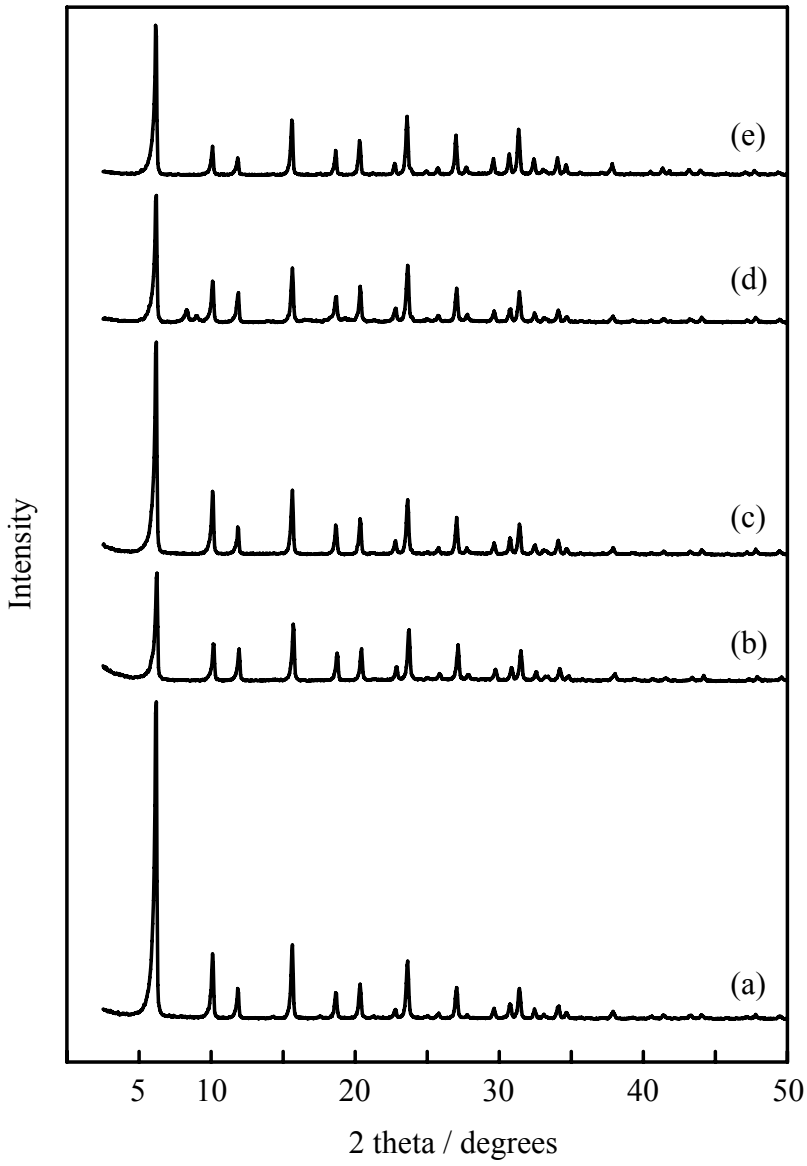

Fig. 3

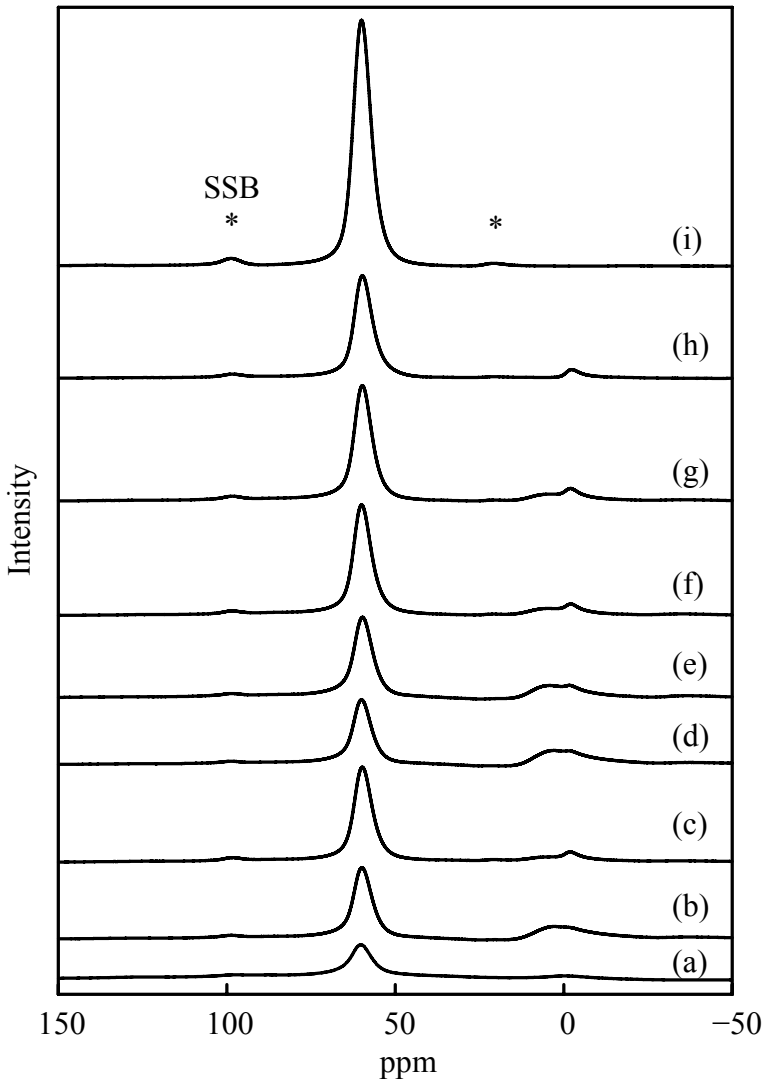

Fig. 4

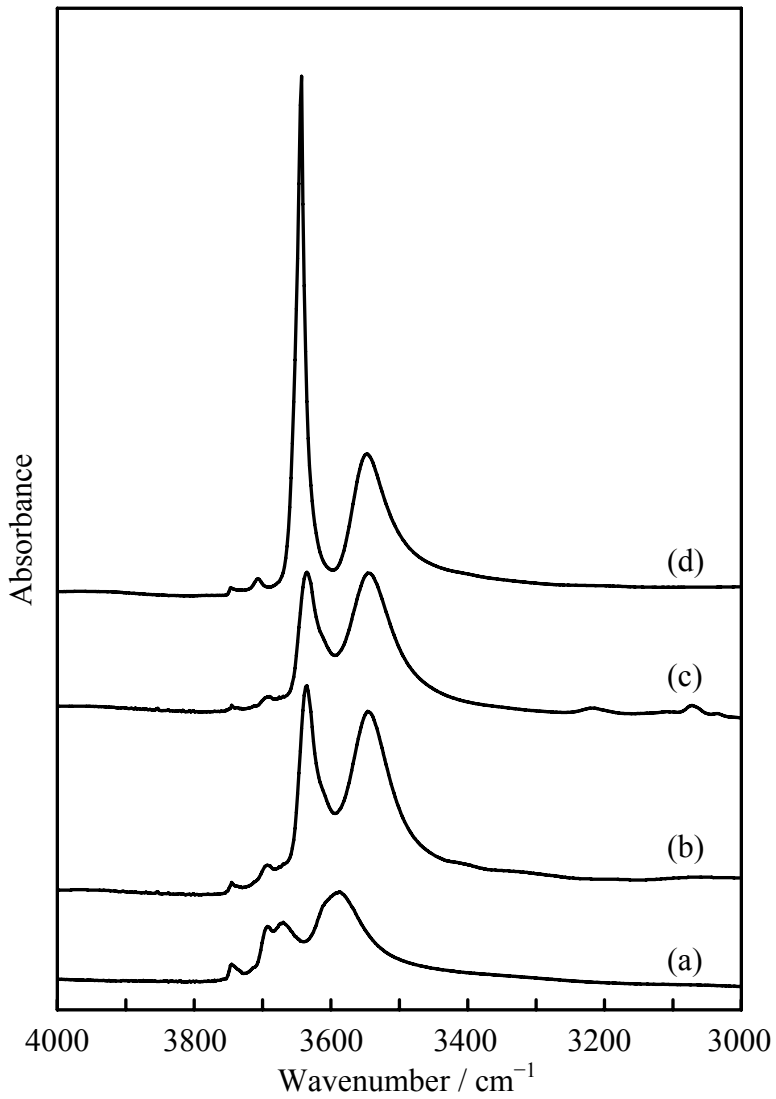
Absorbance
(d)
(c)
(b)
(a)
4000
3800
3600
3400
3200
3000
Wavenumber / cm^{-1}

Fig. 5

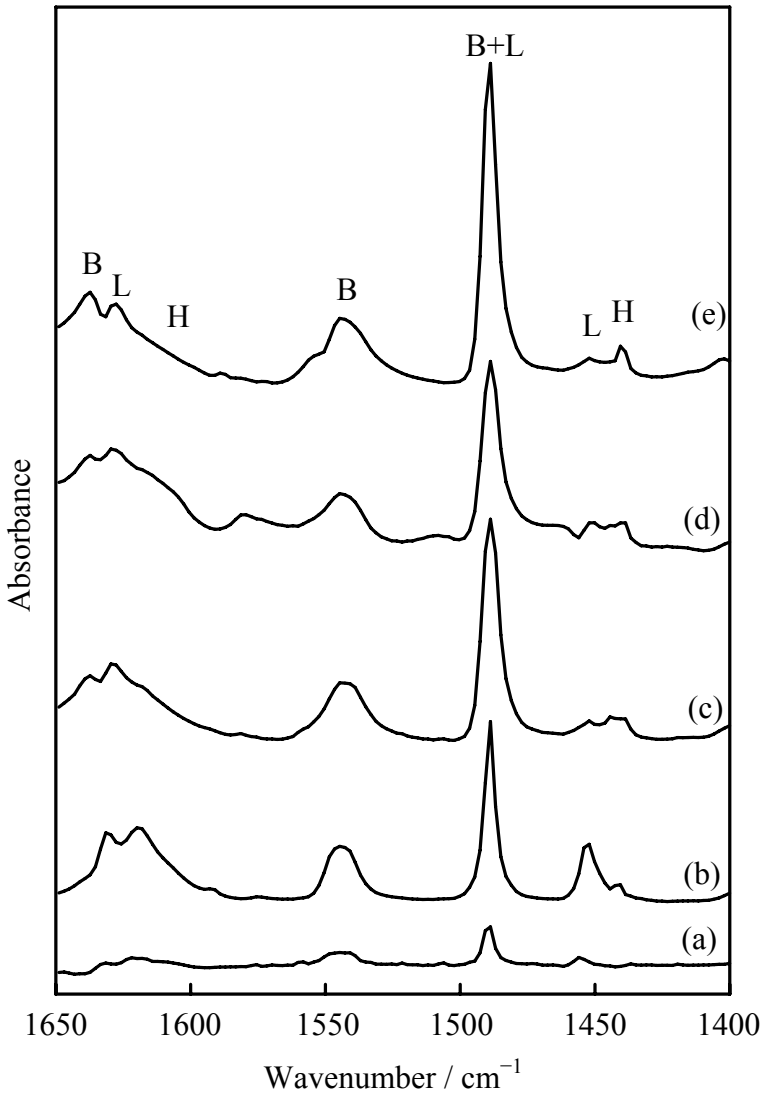
B+L
B
L
H
B
L
H
(e)
(d)
(c)
(b)
(a)
Absorbance
1650
1600
1550
1500
1450
1400
Wavenumber / cm^{-1}

Fig. 6

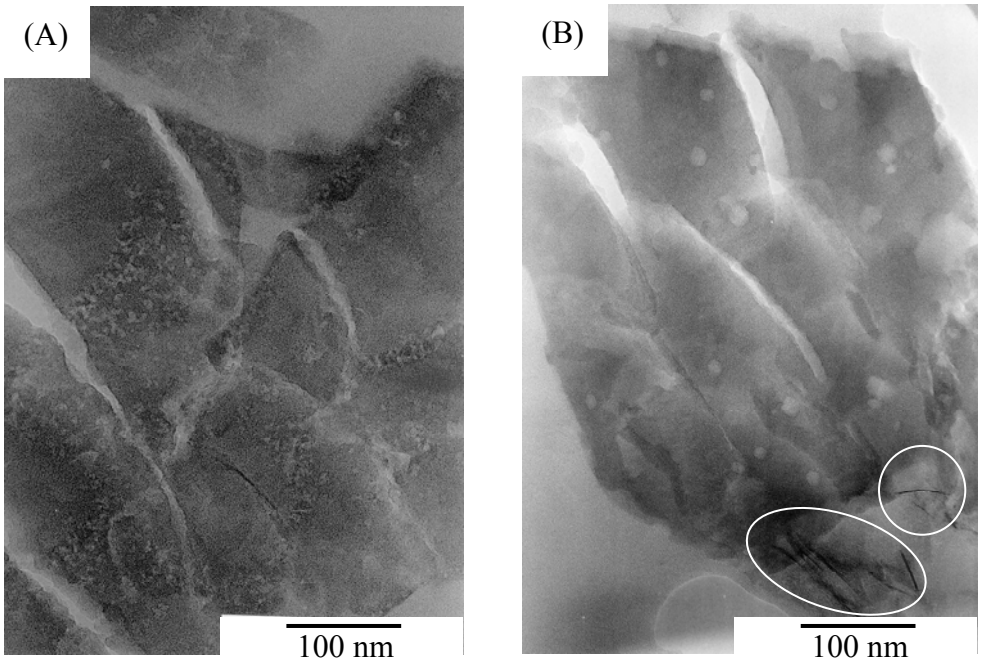

Fig. 7

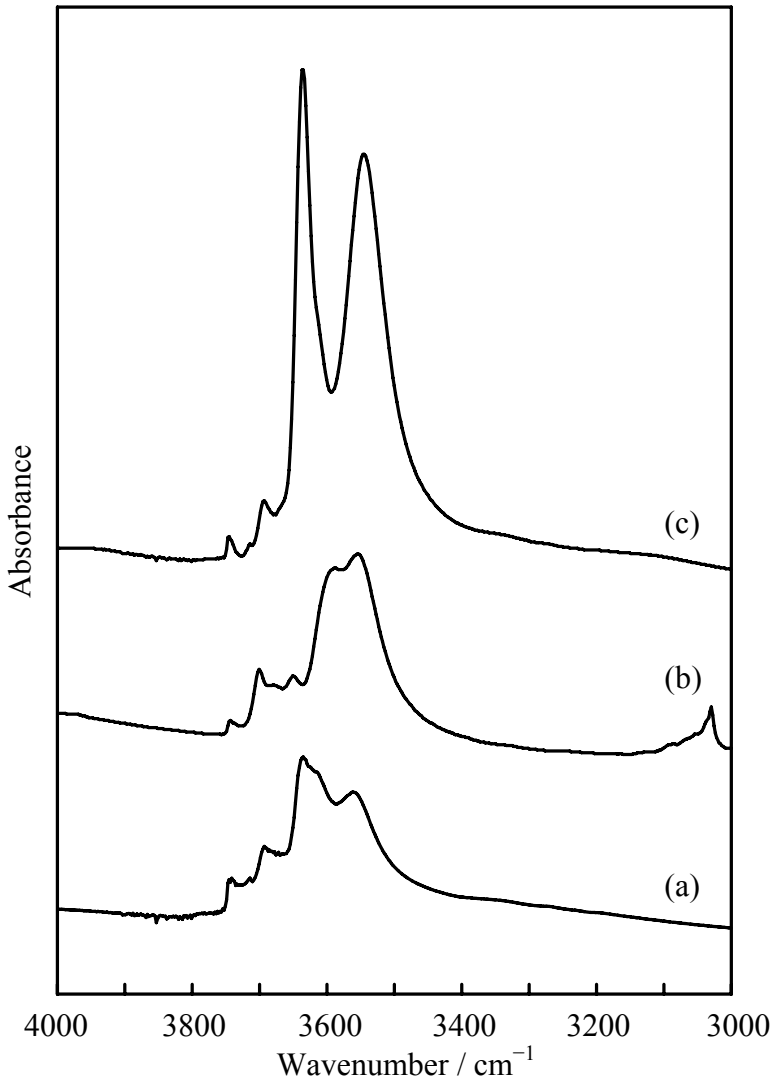
Absorbance
(c)
(b)
(a)
4000
3800
3600
3400
3200
3000
Wavenumber / cm^{-1}

Fig. 8